Wear 350-351 (2016) 82–88

Contents lists available at ScienceDirect

Wear

journal homepage: www.elsevier.com/locate/wear

Influence of TiN coating thickness on the rolling contact fatigue resistance of austempered ductile iron

Diego Alejandro Colombo [a,b,*], María Dolores Echeverría [a,b], Ricardo Cesar Dommarco [b], Juan Miguel Massone [b]

[a] Mechanical Technology Group, School of Engineering, Universidad Nacional de Mar del Plata, Av. J. B. Justo 4302, B7608FDQ Mar del Plata, Argentina
[b] Metallurgy Division, INTEMA – CONICET, Av. J. B. Justo 4302, B7608FDQ Mar del Plata, Argentina

ARTICLE INFO

Article history:
Received 13 October 2015
Received in revised form
13 January 2016
Accepted 17 January 2016
Available online 25 January 2016

Keywords:
Austempered ductile iron
Physical vapor deposition
Titanium nitride
Coating thickness
Rolling contact fatigue

ABSTRACT

The influence of TiN coating thickness on the rolling contact fatigue (RCF) behavior of austempered ductile iron (ADI) was investigated. Coatings were applied in an industrial PVD reactor using processing parameters specifically selected for ADI. Deposition times were adjusted to obtain nominal thicknesses of 0.7, 1.4 and 2.1 μm. RCF tests were performed in a flat washer type testing rig under a lubricated contact. The maximum Hertz contact pressure was 1400 MPa. RCF data were analyzed using the two-parameter Weibull distribution. The rolling track of the tested samples was examined by using SEM. As coating thickness increases, within the analyzed range, the arithmetic average roughness of the coated samples increases slightly while the bearing area decreases more significantly. The elastic modulus and residual stresses of the coatings also increase with thickness, but the coating hardness and the adhesion strength does not. Finally, the RCF resistance of the coated samples decreases as thickness increases. A coating thickness of about 0.7 μm enhances the RCF resistance of ADI substrates while thicker coatings worsen it. Failures in samples with a coating thickness of about 0.7 μm occurred exclusively by substrate spalling, while failures in samples with thicker coatings were mainly produced by coating delamination.

1. Introduction

During the last decades there have been important advances in the study of the mechanical properties and corrosion resistance of austempered ductile iron (ADI) coated with hard coatings by physical vapor deposition (PVD) [1–6]. However, the bibliographic data referred to the wear behavior of PVD coated ADI are very scarce. One of them is the work of Hsu et al. [7] who studied the abrasive and erosive behavior of ADI samples coated with electroless nickel (EN) and PVD-CrTiAlN coatings, finding that the duplex coatings using EN as an interlayer reduce the friction coefficient of ADI and provide a performance against erosive wear better than that of the monolithic EN or CrTiAlN coatings.

More recently, Colombo et al. [8,9] studied the rolling contact fatigue (RCF) and sliding wear behaviors of PVD TiN and CrN coated ADI (about 2.5 μm thick). In addition, the influence of the substrate surface finishing method (polishing and grinding) was also evaluated. With respect to the sliding wear behavior, it was found that the application of both coatings materials reduces to almost zero the wear rate of ADI regardless of the substrate finishing method, while only the application of CrN reduces the friction coefficient of ADI. Regarding the RCF behavior in tests conducted at a maximum Hertz contact pressure, $p_0 = 1400$ MPa, the uncoated ADI performed better than the coated variants while the use of grinding as a substrate finishing method always turned out in longer lives than polishing. Failures observed in coated ADI occurred primarily by coating fracture and delamination promoted by the graphite nodules at the substrate surface.

Studies conducted by other authors related to the RCF behavior of steels coated with different materials by PVD indicate that the coating thickness has a significant influence on the wear resistance [10–21]. For $p_0 < 1100$ MPa, the RCF life of steel samples is enhanced by applying coatings of up to 2 μm thick, while for higher contact pressures the coating thickness should be lower than 1 μm in order to be effective.

Thus, taking into account the aforementioned background, this work studies the influence of the TiN coating thickness on the RCF behavior of ADI with the aim of improving its wear resistance.

* Corresponding author at: Mechanical Technology Group, School of Engineering, Universidad Nacional de Mar del Plata, Av. J. B. Justo 4302, B7608FDQ Mar del Plata, Argentina. Tel.: +54 223 481 6600x260.
E-mail address: diegocolombo@fi.mdp.edu.ar (D.A. Colombo).

http://dx.doi.org/10.1016/j.wear.2016.01.009
0043-1648/

2. Experimental procedures

2.1. Substrate material and samples preparation

The experimental ductile iron used in this work was poured into horizontal gating system sand moulds designed to obtain 70 mm in diameter and 10 mm in thickness discs. The chemical composition of the iron in wt%, analyzed by an optical emission spectrometer, was 3.35% C; 2.87% Si; 0.13% Mn; 0.015% S; 0.032% P; 0.043% Mg; 0.76% Cu; 0.57% Ni and Fe balanced. The nodule count of the discs was about 500 nod/mm^2, with an average nodule diameter of 30 μm. Nodularity exceeded 90% in all cases according to the ASTM A247 standard. The discs were cut from the castings and machined to a final size of 65 mm in diameter and about 8 mm in thickness. According to a previous study [8], an austempering temperature of 280 °C was adopted in order to obtain a high resistance ADI. The heat treatment consisted in: (1) austenitising at 910 °C for 120 min, (2) austempering in a salt bath at 280 °C for 90 min, and (3) air cooling to room temperature, obtaining an average Brinell Hardness of 420 $HBW_{2.5/187.5}$. After the austempering treatment, the samples were ground on a horizontal-spindle (peripheral) surface grinder using industrial-use cutting conditions. Three roughing passes and one finishing pass were performed on each sample in order to attain a low surface roughness.

2.2. PVD coating process

All the substrates were thoroughly degreased, ultrasonically cleaned, rinsed with alcohol and dried with warm air prior to coating deposition. TiN coatings were applied by arc ion plating (AIP) using an industrial reactor and processing parameters specifically selected for ADI. Inside the reactor, and prior to deposition, a bombardment of the substrates with energetic Ti ions was carried out to clean the surface and ensure a good adhesion of the coatings. Table 1 lists the main process parameters utilized. The deposition times were adjusted to obtain three different nominal thicknesses: 0.7 μm (30 min), 1.4 μm (60 min) and 2.1 μm (150 min). The coated samples were identified as “ADI-TiN 0.7”, “ADI-TiN 1.4” and “ADI-TiN 2.1”, respectively.

2.3. Substrates and coatings characterization

Optical microscopy was utilized to identify the microstructure of ADI substrates before and after coating deposition. X-ray diffraction (XRD) was used for phase identification and quantification and for residual stress measurements. A Phillips XPERT-PRO diffractometer was employed with Cu Kα radiation ($\lambda = 1.54187$ Å). XRD patterns for phase identification and quantification were recorded in a 2θ range from 30° to 90° in steps of 0.02° and with a counting time of 1 second per step. Residual stress measurements were conducted using the $\sin^2\psi$ method, with the assumption of a biaxial stress state. Fe-α (222) and TiN (422) reflections were used to measure the strains in the uncoated and coated samples, respectively. The 2θ angle ranged from 120° to 132° for TiN and from 134° to 140° for Fe-α, with a 2θ step of 0.05° and a collection time of 5 s per step. A stylus profilometer (Taylor Hobson Surtronic 3+) with a 4 mm evaluation length (cut off, 0.8 μm) was used to measure the arithmetic average roughness (R_a) and the skewness (R_{sk}) of the uncoated and coated samples. The skewness quantifies the symmetry of the profile about the mean line. A positive skewness is related to a roughness profile with high peaks or shallow valleys while a negative skewness is related to a profile with deep valleys or low peaks. Consequently, a more negative skewness can be associated with a larger bearing area, and vice versa. SEM (JEOL JSM-6460LV) was employed to determine the thickness of the coatings on fractured samples. A microindentation tester equipped with a Knoop indenter was used to measure the surface hardness (15 g load) of the uncoated samples. Instrumented indentation was utilized to measure the hardness and elastic modulus of the coatings. A Hysitron TI 900 Triboindenter device equipped with a Berkovich indenter was employed. Indentations were performed under applied loads of 5.8, 15 and 29 mN for coating thicknesses of 0.7, 1.4 and 2.1 μm, respectively. These loads fulfilled the 1/10th requirement, i.e., the specimen thickness was at least 10 times greater than the indentation depth. A TiN Poisson's ratio of 0.25 was assumed to calculate the elastic modulus [22]. For comparison, the surface (Knoop) hardness of the coated samples was also measured using a 15 g load. A universal hardness tester was employed to evaluate the coating adhesion strength by means of the Rockwell-C adhesion test (150 kg load, VDI 3198 standard) [23].

Table 1
Deposition parameters of TiN coatings.

Substrate-target distance (mm)	200
Substrate BIAS voltage (V)	−175
Arc current (A)	60
Chamber pressure (Pa)	2
Substrate temperature (°C)	300

2.4. Rolling contact fatigue tests

RCF tests were performed in a flat washer type testing rig under a lubricated contact, as schematized in Fig. 1. A commercial SKF 51107 thrust ball bearing was used as a counterpart. This bearing has 21 balls made of SAE 52100 steel with 6 mm in diameter and a rolling diameter of 44 mm. The rotational speed of the samples was set at 1650 rpm, determining a loading frequency of 1.04×10^6 cycles/hour. Lubrication was achieved by immersion of the system in an oil bath with magnetic filtration. A commercial Shell Tellus 100 hydraulic oil was used as lubricant. This oil has a kinematic viscosity of 100 cSt at 40 °C and a density of 0.891 kg/l at 15 °C. The p_0 value was set at 1400 MPa following the results of a previous work [8]. The required normal loads were calculated according to the elastic Hertz theory, taking into account that plastic deformations produced on the samples are negligible [8]. For the uncoated samples, the normal load turned out to be 260 N. According to a previous research [8], this value is also the required for the coated samples.

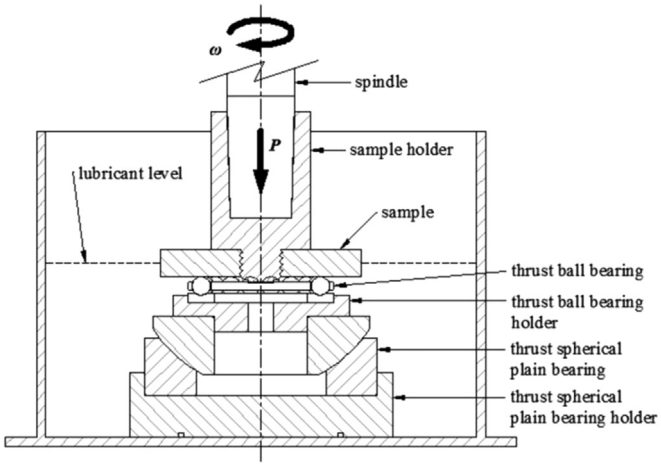

Fig. 1. Schematic view of the flat washer RCF testing rig.

The test conditions produced a minimum oil film thickness, $h_0 = 0.31$ μm, as calculated by using the Hamrock and Dowson equation [24]. The specific oil film thickness parameter (λ) of the uncoated and coated samples ranged from 1.23 to 1.62, resulting in a mixed lubrication regime where the surfaces are separated by a thin lubricant film but asperity contact also takes place.

Six RCF tests were carried out for each material variant. The samples were loaded until a macroscopic fatigue failure was produced on their surface. The life to failure of the samples was measured by an hour meter and converted into loading cycles. Fatigue tests results were analyzed using the two-parameter Weibull distribution. When a test exceeded 100 h without failures, the machine was stopped resulting in a suspended datum that was also taken into account for the analysis. Finally, the rolling track (RT) of the samples was examined by SEM.

3. Results and discussion

3.1. Substrate and coatings characteristics

Fig. 2 contrasts the microstructure of ADI close to the substrate surface before and after the 150 min coating deposition. It can be seen that the microstructure of the coated substrate is analogous to the uncoated one; both composed of acicular ferrite and retained austenite of high carbon content besides graphite nodules. Additionally, the amount of retained austenite and the surface hardness in the substrates was maintained close to 19 vol% and 710 $HK_{0.015}$, respectively, before and after coating depositions. Therefore, it can be said that the coatings processes did not deteriorate the microstructure of ADI substrates.

The diffraction patterns of the uncoated and coated samples are illustrated in Fig. 3. According to the characteristic microstructure of ADI, the patterns of the uncoated samples show the main diffraction peaks of ferrite (Fe-α) and austenite (Fe-γ) phases. The patterns of the coated samples revealed the main diffraction peaks

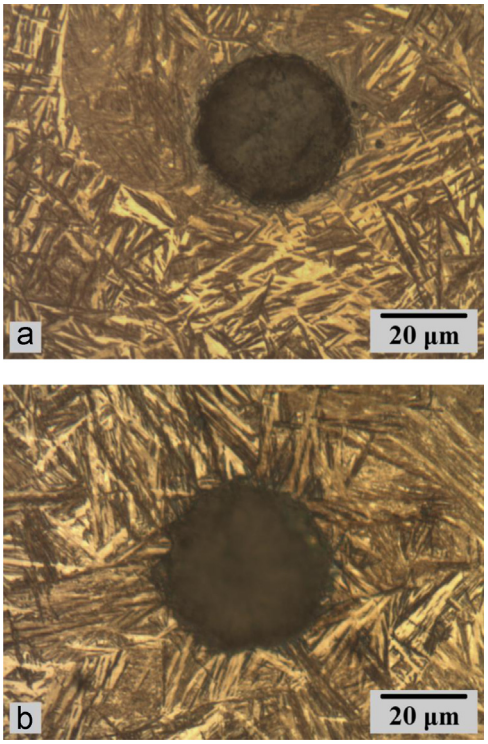

Fig. 2. Microstructure of ADI: (a) before deposition, (b) after a coating deposition of 150 min.

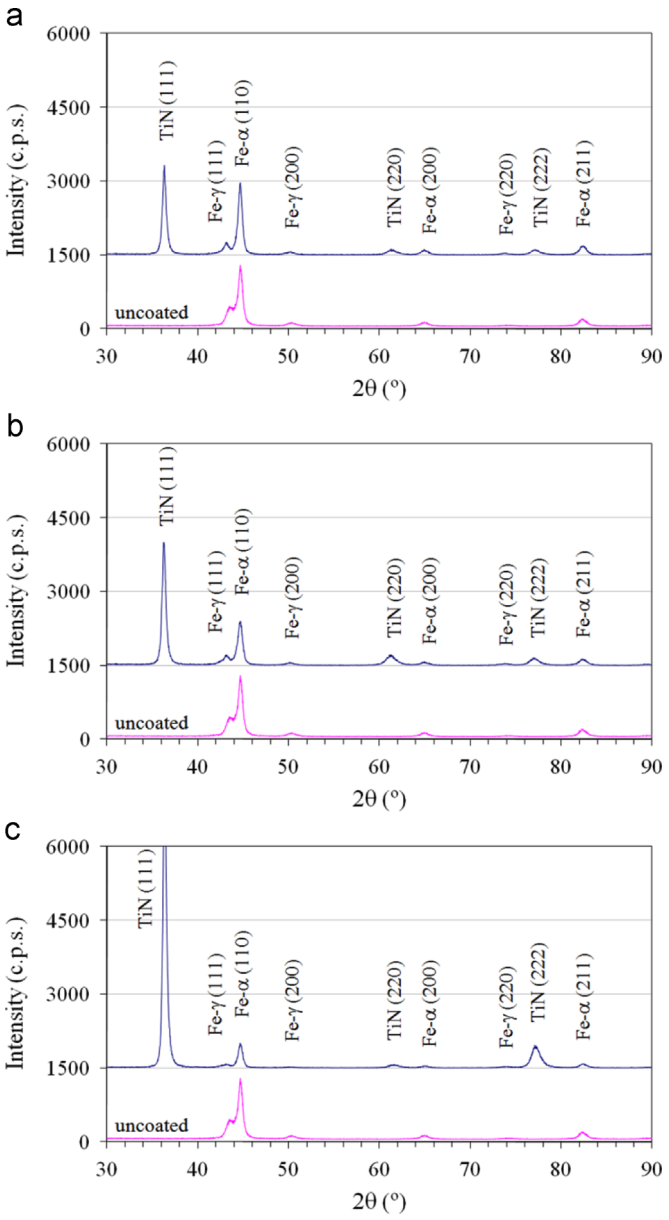

Fig. 3. DRX patterns of uncoated and coated samples: (a) ADI-TiN 0.7, (b) ADI-TiN 1.4, and (c) ADI-TiN 2.1.

of TiN, which correspond to the (111), (220) and (222) planes, together with some substrate peaks. From Fig. 3, it can be seen an increase in the relative intensity of the TiN peaks as coating thickness increases.

The properties of the uncoated and coated samples in terms of coating thickness, surface roughness, hardness, elastic modulus and residual stresses are listed in Table 2.

ADI substrates exhibit average R_a and R_{sk} values of 0.19 μm and −0.28, respectively, a surface hardness of 709 $HK_{0.015}$ and a residual stress value of −0.38 GPa (compression). These results are consistent with a previous study [8].

The average coating thicknesses obtained were 0.75, 1.47 and 2.08 μm for deposition times of 30, 60 and 150 min, respectively. Fig. 4 shows a SEM cross-sectional view of a fractured coated sample, showing the coating with its characteristic columnar morphology and the presence of macroparticles and macro particle voids.

Table 2
Properties of the uncoated and coated samples.

Sample	Coating thickness (μm)	Surface roughness		Coating hardness (GPa)	Surface hardness ($HK_{0.015}$)	Elastic modulus (GPa)	Residual stresses (GPa)
		R_a (μm)	R_{sk}				
ADI	–	0.19 ± 0.02	−0.28 ± 0.26	–	709 ± 30	–	−0.38 ± 0.02
ADI-TiN 0.7	0.75 ± 0.09	0.23 ± 0.02	−0.23 ± 0.25	26.7 ± 2.20	1209 ± 273	329 ± 46	−5.31 ± 0.16
ADI-TiN 1.4	1.47 ± 0.16	0.24 ± 0.03	−0.11 ± 0.26	27.1 ± 1.78	1516 ± 199	395 ± 16	−6.53 ± 0.18
ADI-TiN 2.1	2.08 ± 0.27	0.25 ± 0.03	0.27 ± 0.31	26.3 ± 1.68	2694 ± 164	542 ± 12	−9.18 ± 0.21

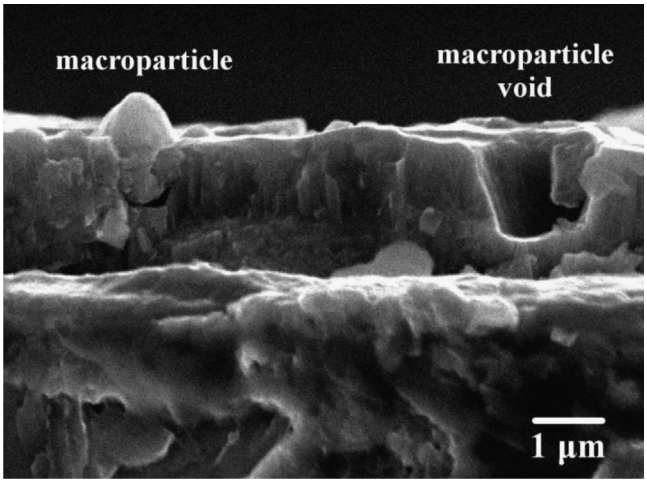

Fig. 4. SEM cross-sectional view of a fractured ADI-TiN 2.1 sample.

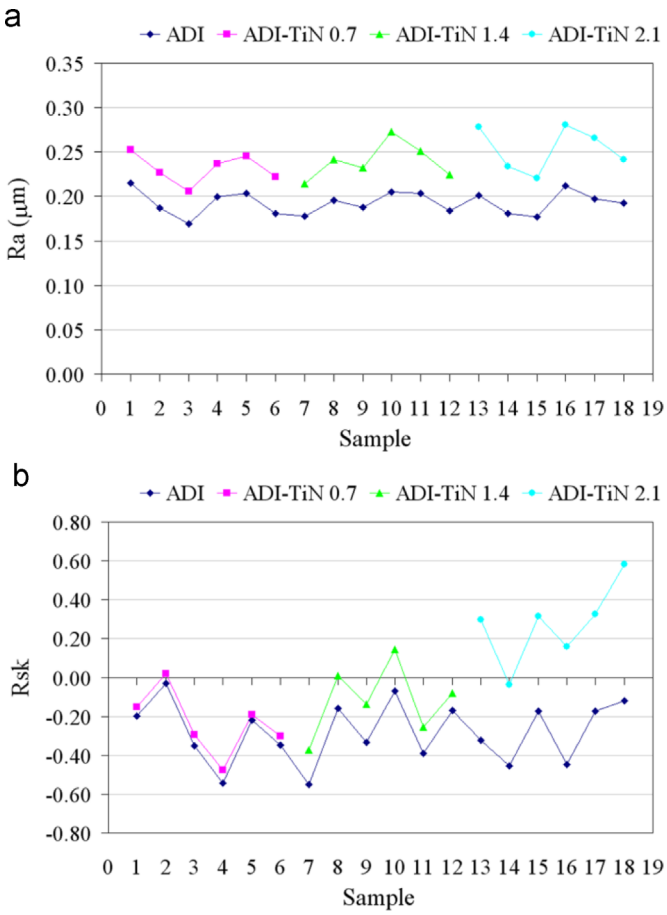

Fig. 5. Roughness parameters of uncoated and coated samples: (a) arithmetic average roughness, (b) skewness.

Regarding the surface roughness, the coated samples exhibit in all the cases a higher R_a and R_{sk} values less negative or even positive than uncoated ADI as can be seen in Fig. 5.

The average R_a values increase slightly as film thickness does, varying from 0.23 μm for ADI-TiN 0.7 to 0.25 μm for ADI-TiN 2.1, while the average R_{sk} values change from −0.23 for ADI-TiN 0.7 to 0.27 for ADI-TiN 2.1. The change in R_{sk} from negative to positive (i.e., the reduction of bearing area) and the slight increase in R_a as coating thickness increases can be ascribed to the presence of macroparticles (protrusions) in the coatings, whose number increases as deposition time does [25].

The coating hardness is close to 27 GPa for the different coating thicknesses analyzed. The surface hardness of ADI-TiN 2.1 (2694 $HK_{0.015}$ = 26.4 GPa) is almost identical to its coating hardness, since the penetration depth of the Knoop indenter is about one tenth of the coating thickness. The surface hardness for smaller coating thicknesses is influenced by the substrate properties.

The elastic modulus and residual stresses of the coatings increase as the coating thickness does. The elastic modulus vary from 329 GPa for ADI-TiN 0.7 to 542 GPa for ADI-TiN 2.1 while the residual stresses vary from −5.31 GPa for ADI-TiN 0.7 to −9.18 GPa for ADI-TiN 2.1, being compressive in all cases.

The adhesion strength of the TiN coatings to ADI substrates was graded as HF1, according to the VDI 3198 Guideline. No delaminations were observed for any of the coating thicknesses analyzed. The imprints resulting from the adhesion tests are shown in Fig. 6.

3.2. Rolling contact fatigue behavior

The analysis of the RCF rolling tracks in the present study show that the failures in the coated samples have different characteristics depending on the coating thickness. In ADI-TiN 0.7, failures occurred exclusively by substrate spalling with no coating damage throughout the samples fatigue life, while in ADI-TiN 1.4 and ADI-TiN 2.1 failures were mainly produced by coating fracture and subsequent delamination with very few cases of substrate spalling. In general, failures produced by coating delamination occurred at fewer loading cycles than those produced by substrate spalling. Fig. 7 shows the two different failure modes described above for the TiN coated samples, substrate spalling in Fig. 7(a) and coating delamination in Fig. 7(b). The rolling direction (RD) is indicated on the micrographs.

Fig. 8 shows the Weibull plot of failure probability versus number of loading cycles for the different coating thicknesses analyzed. The Weibull plot of Fig. 9 compares the failure probability of the uncoated ADI samples with that of the ADI-TiN 0.7 and ADI-TiN 1.4 samples. Table 3 lists the main parameters of the Weibull plots of Figs. 8 and 9 such as L_{10} life, L_{50} life, characteristic life (η) and coefficient of determination (R^2).

From Fig. 8 and Table 3 it can be seen that the RCF life of the coated samples (in terms of loading cycles) increases as the coating thickness decreases. This behavior is consistent with previous studies conducted on steel substrates coated by PVD with different

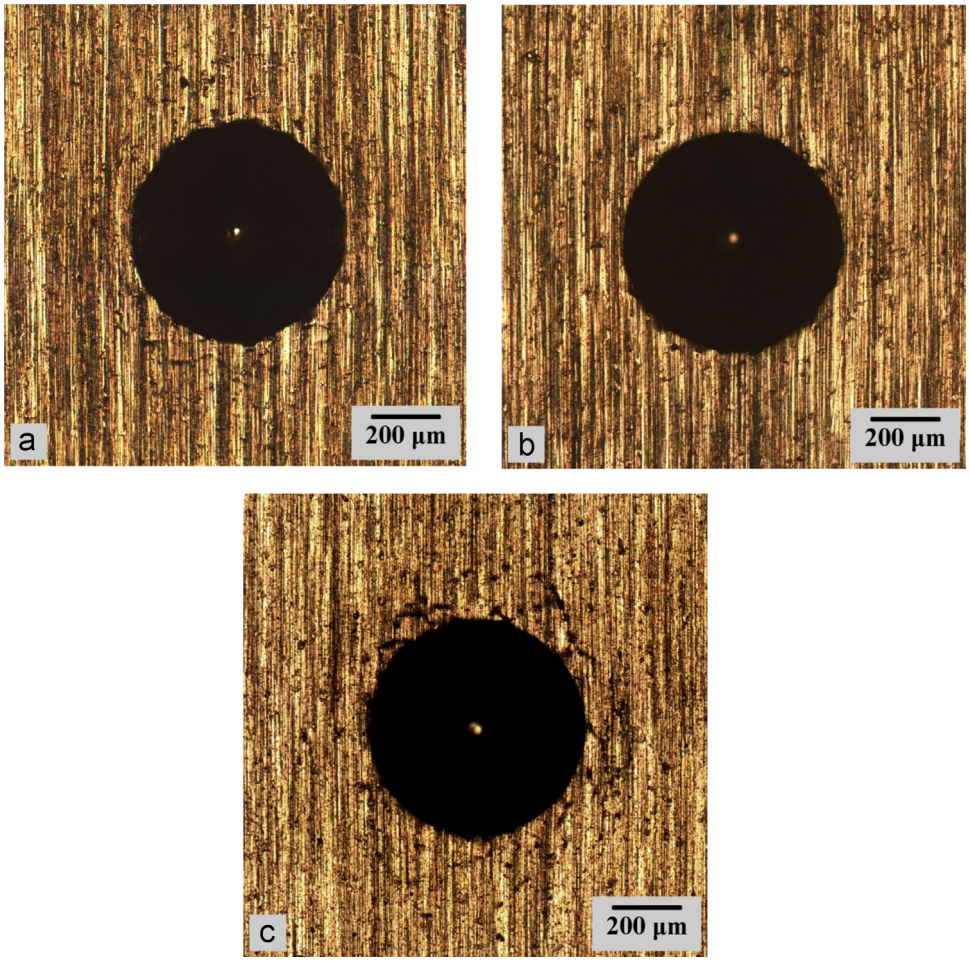

Fig. 6. Imprints on coated samples after Rockwell-C adhesion test (VDI 3198 standard): (a) ADI-TiN 0.7, (b) ADI-TiN 1.4, and (c) ADI-TiN 2.1.

materials [12–15] and can be ascribed to the combination of different facts. First, the reduction of elastic modulus as coating thickness decreases which makes thinner coatings more likely to withstand the deformations experienced by the relatively softer and more compliant substrates during the loading/unloading RCF cycles without cracking and/or delamination [26]. Second, the increase of residual stresses as coating thickness does which makes thicker coatings more likely to suffer fracture and delamination during system use in tribological applications [27]. Third, the presence of larger defects (the interfaces between columns in the coating structure) as coating thickness increases which makes thicker coatings more prone to suffer fracture and delamination since these defects act as preferential sites for crack nucleation [28]. Furthermore, being that the RCF tests were conducted under a mixed lubrication regime, the surface roughness of the coated samples also played an important role. As stated in Section 3.1, the number of protrusions (macroparticles) in the surface of the coated samples increases significantly as film thickness does. Consequently, the interaction between the rolling surfaces also increases as film thickness does, making thicker coatings more likely to fail. The different failure modes observed as coating thickness increases ratify that thinner coatings (less than 1 μm) are more likely to withstand the RCF test without cracking and/or delamination.

From Fig. 9 and Table 3 it can be noted that TiN coatings with a thickness of 0.7 μm enhance the RCF resistance of ADI substrates while those with thicknesses of 1.4 and 2.1 μm worsen ADI's resistance. Particularly, ADI-TiN 0.7 increases the η life of ADI substrates by approximately 26%, while ADI-TiN 1.4 and ADI-TiN 2.1 decrease the η life of ADI substrates by 10% and 27%, respectively. This result is also consistent with previous studies carried out on PVD coated steels, in which it was found that the optimum coating thickness is close to 0.75 μm and that thinner thicknesses do not affect the RCF resistance of the bare substrates [17,20,28].

4. Conclusions

PVD TiN coatings were applied on high strength ADI samples. The influence of the coating thickness on the RCF behavior of the coated samples was studied. Three different coating thicknesses were analyzed: 0.75, 1.47 and 2.08 μm. Based on the results obtained within the thickness range analyzed and the RCF test conditions used, the following conclusions can be drawn:

- The elastic modulus and residual stresses of the coatings increase significantly as coating thickness does. The number of protrusions (macroparticles) in the surface, the arithmetic average roughness and the surface hardness of the coated samples also increase with the coating thickness. The coating hardness and adhesion strength quality do not vary with the thickness. And finally, the RCF resistance of the coated samples decreases as coating thickness increases.
- Samples with a coating thickness of 0.75 μm exhibit a higher RCF resistance than uncoated ADI samples. Failures in these samples are produced exclusively by substrate spalling with no

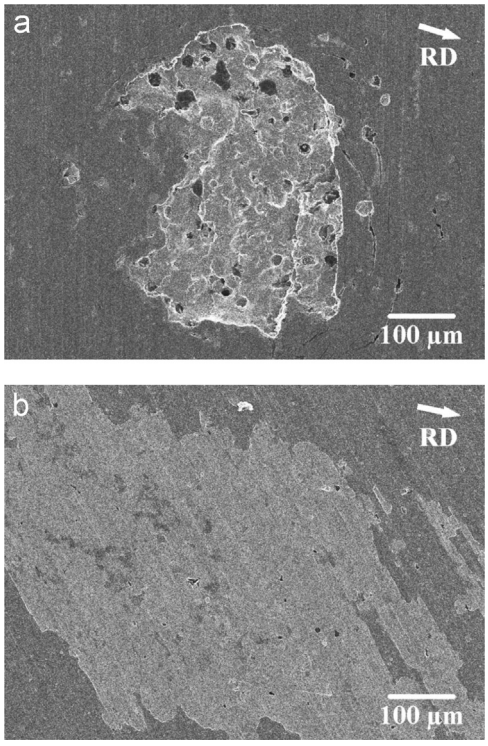

Fig. 7. Different RCF failure modes observed in the TiN coated samples: (a) substrate spalling observed in ADI-TiN 0.7, (b) coating delamination observed in ADI-TiN 1.4 and ADI-TiN 2.1.

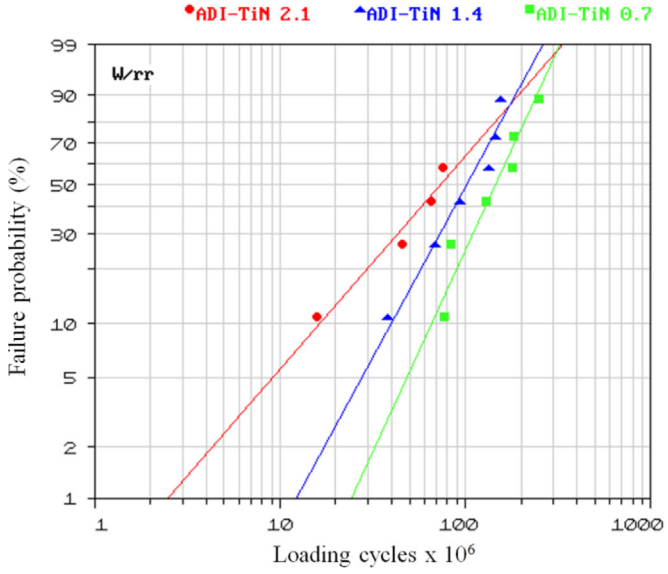

Fig. 8. Weibull plot for the coated samples (p_0=1400 MPa, mixed lubrication regime).

coating damage throughout their fatigue life. Samples with coating thicknesses of 1.47 and 2.08 µm show a lower RCF resistance than uncoated ADI samples. Failures in these samples are mainly produced by coating fracture and subsequent delamination.

- The combined reduction of elastic modulus, residual stresses, defects size and number of protrusions as coating thickness decreases can be ascribed to the enhanced capacity of thinner coatings to withstand the RCF test without cracking and/or delamination.

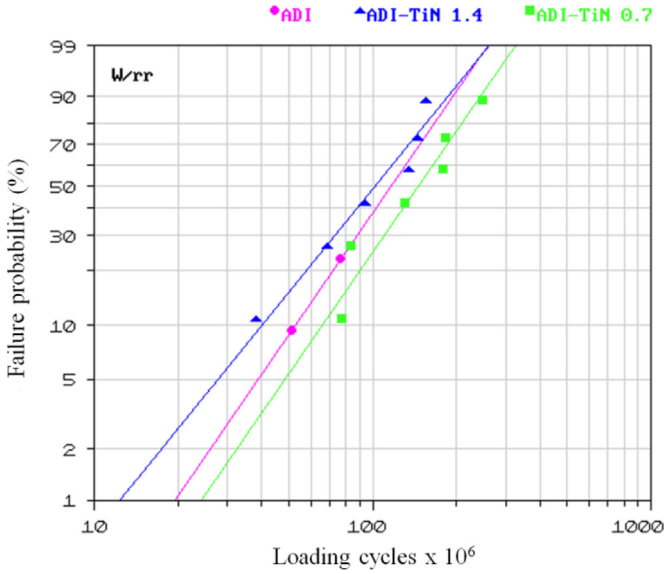

Fig. 9. Failure probability for uncoated ADI compared to ADI-TiN 0.7 and ADI-TiN 1.4 (p_0=1400 MPa, mixed lubrication regime).

Table 3
Typical values of the FCR resistance curves for the uncoated and coated samples.

Sample	L_{10} (cycles × 10^6)	L_{50} (cycles × 10^6)	η (cycles × 10^6)	R^2
ADI	52.547	116.135	135.510	0.999
ADI-TiN 0.7	65.687	145.952	170.479	0.926
ADI-TiN 1.4	39.727	101.978	122.507	0.956
ADI-TiN 2.1	16.250	73.500	98.583	0.955

Acknowledgments

The authors wish to thank the company Sudosilo S.A. for its generous collaboration in coatings deposition. The financial support granted by the CONICET (Grant No. PIP 11220110100558) and the National University of Mar del Plata (Grant No. 15/G394) is also gratefully acknowledged.

References

[1] H.P. Feng, S.C. Lee, C.H. Hsu, J.M. Ho, Study of high cycle fatigue of PVD surface-modified austempered ductile iron, Mater. Chem. Phys. 59 (1999) 154–161.
[2] C.H. Hsu, J.K. Lu, K.L. Lai, M.L. Chen, Erosion and corrosion behaviors of ADI deposited TiN/TiAlN coatings by cathodic arc evaporation, Mater. Trans. 46 (2005) 1417–1424.
[3] C.H. Hsu, M.L. Chen, K.L. Lai, Corrosion resistance of TiN/TiAlN-coated ADI by cathodic arc deposition, Mater. Sci. Eng. A 421 (2006) 182–190.
[4] C.H. Hsu, C.Y. Lee, K.L. Chen, J.H. Lu, Effects of CrN/EN and Cr2O3/EN duplex coatings on corrosion resistance of ADI, Thin Solid Films 517 (2009) 5248–5252.
[5] C.H. Hsu, K.L. Chen, C.Y. Lee, K.C. Lu, Effects of low-temperature duplex coatings on corrosion behavior of austempered ductile iron, Surf. Coat. Technol. 204 (2009) 997–1001.
[6] C.H. Hsu, K.H. Huang, Y.T. Chen, W.Y. Ho, The effect of electroless Ni–P interlayer on corrosion behavior of TiN-coated austempered ductile iron, Thin Solid Films 529 (2013) 34–38.
[7] C.H. Hsu, K.L. Chen, K.C. Lu, Effects of low-temperature duplex coatings on the abrasive and erosive behavior of ADI, Thin Solid Films 519 (2011) 4855–4859.
[8] D.A. Colombo, M.D. Echeverría, S. Laino, R.C. Dommarco, J.M. Massone, Rolling contact fatigue resistance of PVD CrN and TiN coated austempered ductile iron, Wear 308 (2013) 35–45.
[9] D.A. Colombo, M.D. Echeverría, S. Laino, R.C. Dommarco, J.M. Massone, Sliding wear behavior of PVD CrN and TiN coated austempered ductile iron, ISIJ Int. 54 (2014) 2860–2867.
[10] J.F. Dill, M.N. Gardos, H.E. Hintermann, H.J. Boving, Rolling contact fatigue evaluation of hard coated bearing steels, In: Proceedings of the Third International Conference on Solid Lubrication, Denver, Colorado, USA, 1984, pp. 230–241.

[11] R.F. Hochman, A. Erdemir, F.J. Dolan, R.L. Thom, Rolling contact fatigue behavior of Cu and TiN coatings on bearing steel substrates, J. Vac. Sci. Technol. A: Vac. Surf. Films 3 (1985) 2348–2353.
[12] A. Erdemir, R.F. Hochman, Tribological behaviour of ion-plated TiN coatings under sliding and rolling contact, In: Proceedings of the Conference on Ion Implantation and Plasma-Assisted Processes for Industrial Applications, Atlanta, Georgia, USA, 1988.
[13] T.S.P. Chang, H.S. Cheng, W.D. Sproul, The influence of coating thickness on lubricated rolling contact fatigue life, Surf. Coat. Technol. 43–44 (1990) 699–708.
[14] H.S. Cheng, T.P. Chang, W.D. Sproul, A morphological study of contact fatigue of TiN coated rollers, In: Proceedings of the 16th Leeds-Lyon Symposium on Tribology, Lyon, France, 1990, pp. 81–88.
[15] T.P. Chang, H.S. Cheng, W.A. Chiou, W.D. Sproul, Comparison of fatigue failure morphology between TiN coated and uncoated lubricated rollers, Tribol. Trans. 34 (1991) 408–416.
[16] R. Wei, P.J. Wilbur, F.M. Kustas, A. Rolling, Contact fatigue study of hard carbon coated M-50 steel, J. Tribol. 114 (1992) 298–302.
[17] R. Thom, L. Moore, W.D. Sproul, T. Peter Chang, Rolling contact fatigue tests of reactively sputtered nitride coatings of Ti, Zr, Hf, Cr, Mo, Ti–Al, Ti–Zr and Ti–Al–V on 440C stainless steel substrates, Surf. Coat. Technol. 62 (1993) 423–427.
[18] R. Wei, P.J. Wilbur, M.J. Liston, Effects of diamond-like hydrocarbon films on rolling contact fatigue of bearing steels, Diamond Relat. Mater. 2 (1993) 898–903.
[19] A. Sawamoto, S. Nokubo, Y. Ide, T. Fujita, T. Fukui, K. Yasuoka, Influence of TiN coating on the rolling contact fatigue strength of mild steel, J. Soc. Mater. Sci. Jpn 45 (1996) 912–918.
[20] Y.H. Chen, I.A. Polonsky, Y.W. Chung, L.M. Keer, Tribological properties and rolling-contact-fatigue lives of TiN/SiN_x multilayer coatings, Surf. Coat. Technol. 154 (2002) 152–161.
[21] D. Yonekura, R.J. Chittenden, P.A. Dearnley, Wear mechanisms of steel roller bearings protected by thin, hard and low friction coatings, Wear 259 (2005) 779–788.
[22] H. Ljungcrantz, M. Oden, L. Hultman, J.E. Greene, J.E. Sundgren, Nanoindentation studies of single-crystal (001)-, (011)-, and (111)-oriented TiN layers on MgO, J. Appl. Phys. 80 (1996) 6725–6733.
[23] W. Heinke, A. Leyland, A. Matthews, G. Berg, C. Friedrich, E. Broszeit, Evaluation of PVD nitride coatings, using impact, scratch and Rockwell-C adhesion tests, Thin Solid Films 270 (1995) 431–438.
[24] B.J. Hamrock, D. Dowson, Isothermal elastohydrodynamic lubrication of point contacts: Part III-Fully Flooded Results, J. Lubr. Technol. 99 (1977) 264–275.
[25] C.N. Tai, E.S. Koh, K. Akari, Macroparticles on TiN films prepared by the arc ion plating process, Surf. Coat. Technol. 43–44 (Part 1) (1990) 324–335.
[26] A. Erdemir, R.F. Hochman, Surface metallurgical and tribological characteristics of TiN-coated bearing steels, Surf. Coat. Technol. 36 (1988) 755–763.
[27] S.J. Bull, Can scratch testing be used as a model for the abrasive wear of hard coatings? Wear 233–235 (1999) 412–423.
[28] I.A. Polonsky, T.P. Chang, L.M. Keer, W.D. Sproul, A study of rolling-contact fatigue of bearing steel coated with physical vapor deposition TiN films: coating response to cyclic contact stress and physical mechanisms underlying coating effect on the fatigue life, Wear 215 (1998) 191–204.